Int. J. Heat Mass Transfer. Vol. 30, No. 5, pp. 833–841, 1987
Printed in Great Britain

0017–9310/87 $3.00 + 0.00
Pergamon Journals Ltd.

Mixed convection heat transfer in horizontal, concentric annuli for transitional flow conditions

M. CIAMPI, S. FAGGIANI, W. GRASSI and G. TUONI
Dipartimento di Energetica, Universita degli Studi di Pisa, 56100 Pisa, Via Diotisalvi 2, Italy

and

F. P. INCROPERA
School of Mechanical Engineering, Purdue University, West Lafayette, Indiana, U.S.A.

(*Received* 24 *April* 1986 *and in final form* 28 *August* 1986)

Abstract—Experiments have been performed to determine mixed convection flow and heat transfer in a horizontal, concentric tube annulus for Reynolds numbers in the range $2200 < Re < 5000$. Within this range, flow conditions are turbulent and laminar, respectively, in regions of the annulus above and below the heated inner tube. For Reynolds numbers less than a critical value Re_1, which depends on the Rayleigh number, diameter ratio and longitudinal position, flow along the sides of the annulus is laminar and helicoidal. For $Re > Re_1$, there is a breakdown in the helicoidal motion, with subsequent transition to turbulence in the top and side regions of the annular passage. The local Nusselt number at the top of the inner tube is less than, equal to, and greater than that at the bottom for $Re < Re_1$, $Re = Re_1$, and $Re > Re_1$, respectively. The circumferentially averaged Nusselt number is weakly dependent on longitudinal position and may be correlated in terms of the Rayleigh and Reynolds numbers and the tube diameter ratio.

INTRODUCTION

CONVECTION heat transfer in a concentric tube annulus is pertinent to numerous applications such as the heating of process fluids, the cooling of electrical cables and nuclear fuel rods, and the collection of solar energy. In many of these applications, flow through the annular passage is characterized by small Reynolds numbers for which buoyancy effects may be significant. Such effects are especially pronounced for horizontal flows, where buoyancy driven secondary motion may significantly enhance heat transfer and promote early transition to turbulence.

Although many theoretical and experimental studies of mixed convection have been performed for both horizontal circular tubes and rectangular ducts, comparatively little has been done for the concentric annulus. Most of the existing literature pertains to numerical simulations for laminar, fully developed flow, with uniform heating at either the inner or outer tube [1–5]. At low to moderate Rayleigh numbers, the buoyancy induced secondary flow is predicted to consist of a large roll cell on each side of the vertical midplane. As discussed by Mojtabi and Caltagirone [2], the net effect of the main and secondary flows is to produce a helicoidal motion for which fluid ascends (descends) along the heated (cooled) inner tube and descends (ascends) along the cooled (heated) outer tube, as it moves in the longitudinal direction. The strength of the roll increases with Rayleigh number, until transition occurs from a single to a double roll pattern. With the inner tube heated, the second (weaker) cell was predicted to occur at the top of the annular region by Hattori [1, 5] and at the bottom by Kaviany [3] and Nieckele and Patankar [4]. Appearance of the second cell corresponds to a sharp increase in the circumferentially averaged Nusselt number, with values exceeding those corresponding to forced convection by up to a factor of 3. With increasing Rayleigh number, thermal conditions tended towards stable stratification [3, 4] and longitudinal velocities at the top of the annular region became progressively smaller than those at the bottom.

For the inner tube heated and an assumed uniform temperature around the circumference, the local Nusselt number was predicted to decay monotonically from a maximum at the bottom of the tube ($\theta = 180°$) to a minimum at the top ($\theta = 0°$) [4]. The Nusselt number ratio Nu_b/Nu_t increases with increasing Rayleigh number and decreasing diameter ratio from unity (negligible buoyancy) to approximately six for $Ra^* = 10^7$ and $D_o/D_i = 1.5$. Following the onset of buoyancy effects, Nu_t remains approximately constant and the increase in Nu_b/Nu_t is due primarily to increasing Nu_b. This trend differs somewhat from that predicted by Kaviany [3] for an assumed uniform heat flux around the circumference of the inner tube. Although minimum and maximum wall temperatures, and hence maximum and minimum Nusselt numbers, were predicted for the bottom and top, respectively,

NOMENCLATURE

D	diameter
D_h	hydraulic diameter, $(D_o - D_i)$
G	mass velocity
g	gravitational acceleration
h	local convection coefficient, $q(\theta)/[T_{w,i}(\theta, x) - T_m(x)]$
$\bar{h}$	circumferentially averaged convection coefficient, $\bar{q}/[T_w(x) - T_m(x)]$
k	thermal conductivity
m	coefficient in local Nusselt number correlation
Nu	local Nusselt number, hD_h/k
$\overline{Nu}$	circumferentially averaged Nusselt number, $\bar{h}D_h/k$
Pr	Prandtl number
q	local heat rate per unit area
$\bar{q}$	circumferentially averaged heat rate per unit area
r	radius measured from centerline of inner tube
Ra^*	Rayleigh number, $g\beta Pr\,\bar{q}D_h^4/kv^2$
Re	Reynolds number, $4G/\pi(D_o + D_i)\mu$
T_m	mixed mean fluid temperature
T_w	wall temperature
u	longitudinal velocity
x	longitudinal distance from entrance of heated section.

Greek symbols

β	thermal expansion coefficient
θ	circumferential angle measured from top with center of inner tube as origin
μ	dynamic viscosity
ν	kinematic viscosity.

Subscripts

b	bottom of tube ($\theta = 180°$)
i	inner tube
o	outer tube
t	top of tube ($\theta = 0°$)
1	condition for which $Nu_t = Nu_b$.

the variation of the top temperature with Rayleigh number exhibited a distinct maximum, at first increasing and then decreasing with increasing Ra^*. Appearance of the maximum corresponds to transition from a single to double cellular flow pattern. In any case, the inequality $Nu_t < Nu_b$ is clearly due to the secondary flow, which brings heated fluid to the top of the tube and restores cooler fluid to the bottom.

Experimental studies of mixed convection in a horizontal annulus have been performed for water in fully developed, laminar flow [6, 7]. Hattori and Kotake [6] present and correlate data for the circumferentially averaged Nusselt number, while Ciampi *et al.* [7] present data for the circumferential distribution of the local Nusselt number, as well as correlations for the average Nusselt number. The circumferential measurements of Ciampi *et al.* are consistent with the predictions of Nieckele and Patankar [4] for Nu_b/Nu_t and with the predictions of Kaviany [3] for the variation of $T_{w,i}(\theta = 0°)$ with Ra^*.

The present study is an extension of previous experiments [7] to larger Reynolds numbers corresponding to transitional and turbulent flow conditions. Experiments are performed for water flow in a horizontal annulus with inner tube heated and outer tube insulated. Diameter ratios (D_o/D_i) of 1.65 and 2.18 are considered, along with Reynolds and Rayleigh numbers in the ranges $2200 < Re < 5000$ and $10^7 < Ra^* < 10^9$. Emphasis is placed on determining circumferential variations in the local Nusselt number.

EXPERIMENTAL PROCEDURES

As shown in Fig. 1(a), filtered and metered water is routed from a storage vessel to a horizontal, concentric tube annulus. The inner tube is of fixed diameter ($D_i = 34$ mm) and consists of a 3.4 m long unheated starting section, a 1.4 m long heated section, and a 1.4 m long trailing section. The starting and trailing sections consist of copper rods which are joined to a central stainless steel tube of 3 mm wall thickness. With electric current passed through the rod/tube assembly from a 200 kW d.c. power supply, more than 99.5% of the power per unit length is dissipated in the tube. Since spatial variations in the electrical resistivity of the stainless steel are negligible, the electric power is uniformly dissipated throughout the tube and the rate of dissipation per unit surface area, $\bar{q}$, may be determined from measurement of the tube current and voltage drop. However, due to circumferential variations in the local convection coefficient and tube wall conduction effects, the local convective heat flux $q(\theta)$ will deviate from $\bar{q}$. For most of the conditions of this study, the deviation is small and the assumption is made that $q(\theta) = \bar{q}$. However, under operating conditions for which there are large variations in the local convection coefficient, a corrected heat flux is determined from a procedure which uses measured circumferential variations in the tube wall temperature [7]. The procedure is consistent with the requirement that

$$\bar{q} = (1/\pi)\int_0^\pi q(\theta)\,d\theta.$$

The copper rod in the trailing section is bored to permit passage of 16, 0.05 mm chromel–alumel thermocouples. For each of eight longitudinal stations, two of the thermocouples are joined to the

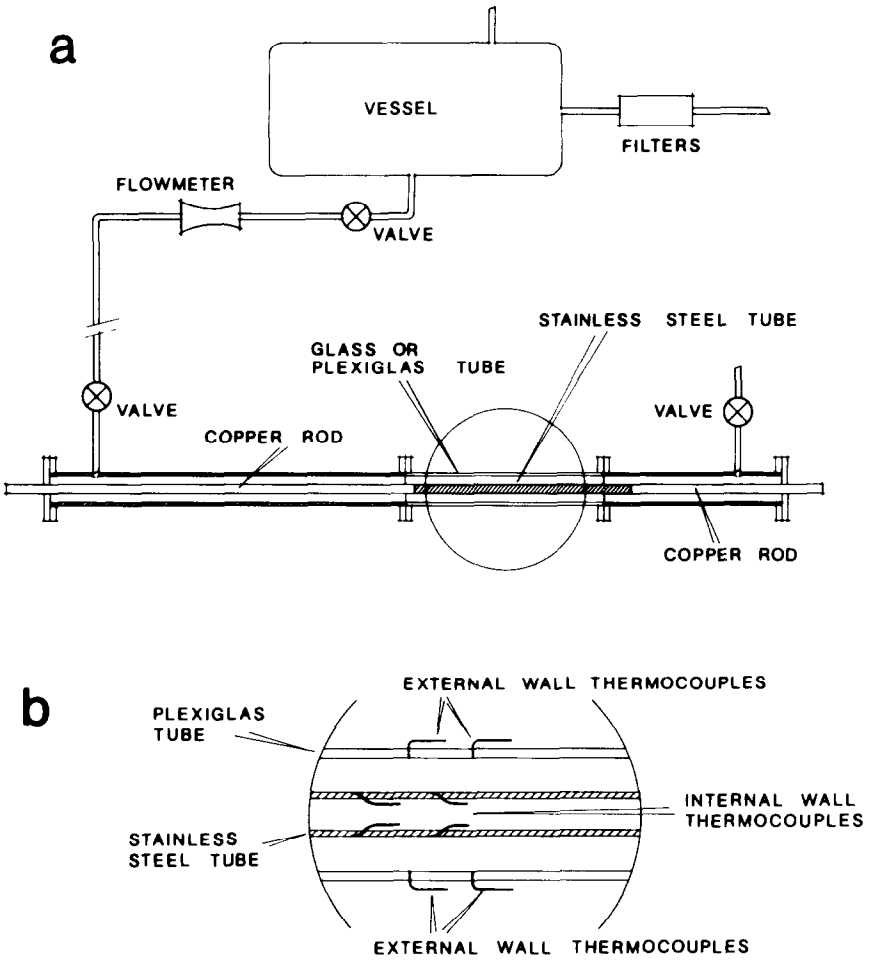

FIG. 1. Experimental facility: (a) flow loop, (b) thermocouple placement.

stainless steel inner tube at circumferential locations which differ by 180° (Fig. 1(b)). The longitudinal spacing between thermocouple pairs ranges from 50 mm near the inlet to 400 mm near the outlet. By rotating the inner tube 90° about its axis, the tube wall temperature may be obtained for 15 values of θ in the range from 0 to 180°.

The outer tube is fabricated from stainless steel, with a plexiglas insert used to facilitate flow visualization for the central (heated) section. The annulus was well insulated from the surroundings, except during flow visualization, when the insulation was removed from the plexiglas section. Two outer tube diameters (56 and 74 mm) were considered, and chromel–alumel thermocouples were used to measure the outer wall temperature. Two thermocouples were used to measure the water inlet temperature, and the longitudinal distribution of the mixed mean water temperature, $T_m(x)$, was determined from energy balance considerations. All thermocouples were separately calibrated.

To within the uncertainty of the temperature measurements ($\pm 2\%$), results obtained for $T_{w,i}$ at the top ($\theta = 0°$) and bottom ($\theta = 180°$) of the tube yielded linearly increasing longitudinal distributions for $x > 0.2$ m, and presentation of the results of this study is restricted to this region. The results are presented in terms of local and average Nusselt numbers defined as

$$Nu = \frac{q(\theta)D_h}{[T_{w,i}(\theta) - T_m]k} \tag{1}$$

$$\overline{Nu} = \frac{\bar{q}D_h}{(T_{w,i} - T_m)k}. \tag{2}$$

In reducing the data, all properties are evaluated at the arithmetic average value of the fluid inlet and outlet temperatures.

At selected longitudinal stations, additional temperature measurements were obtained by radially traversing a thermocouple through the fluid. Also, flow visualization was performed by injecting dye through hypodermic needles located slightly upstream or downstream of the entrance to the heated section. The dye was injected in the streamwise direction at a radial location close to the inner surface or midway between the tube walls and at angular positions of $\theta = 0$ or 180°. The dye was injected either continu-

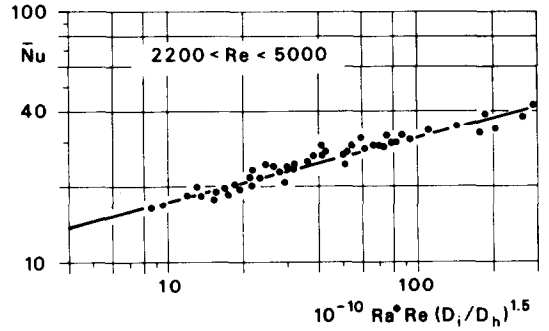

FIG. 2. Circumferentially averaged Nusselt number for the inner tube ($2200 < Re < 5000$; $10^7 < Ra^* < 10^9$; $D_o/D_i = 1.65, 2.18$).

ously (to track the streamline pattern of the flow) or drop by drop (to obtain the longitudinal velocity of the flow). The longitudinal velocity was determined by recording the time required for a droplet to travel a prescribed distance.

EXPERIMENTAL RESULTS

Data for the circumferential average of the inner tube Nusselt number are plotted in Fig. 2 as a function of the parameter $Ra^* Re(D_i/D_h)^{1.5}$. To within the $\pm 10\%$ uncertainty of the measurement procedures, the results were independent of x for $x > 0.2$ m. The data reveal a consistent trend of increasing $\overline{Nu}$ with increasing Ra^*, Re and D_i/D_h and are correlated to within 15% by an expression of the form

$$\overline{Nu} = 0.0274(Re\,Ra^*)^{0.25}(D_i/D_h)^{0.38}. \quad (3)$$

Unlike previous results obtained for laminar flow [7], there is now a clear dependence of $\overline{Nu}$ on Re. The fact that the Reynolds number exponent (0.25) is much smaller than that for fully turbulent forced convection is consistent with the transitional nature of the flow. The Rayleigh number exponent (0.25) is consistent with that corresponding to free convection from a horizontal cylinder in an infinite quiescent fluid [8] or from the inner tube of a concentric annulus [9].

Although no unusual trends are associated with the effect of Reynolds number on the average Nusselt number, the circumferential distribution of the local Nusselt number is radically altered by variations in the Reynolds number. The nature of this alteration is shown in Figs. 3 and 4, where representative data for the longitudinal distribution of the top and bottom inner tube temperatures and Nusselt numbers are plotted for different values of Re. The distributions for $Re = 2380$, which are characterized by $T_t > T_b$ and $Nu_t < Nu_b$ for all x, are typical of those obtained at lower Reynolds numbers. However, with increasing Re, the distributions intersect, with $T_b > T_t (Nu_b < Nu_t)$ for small x and $T_t > T_b (Nu_t < Nu_b)$ for large x. This behavior is shown in Figs. 3(b) and 4(b) and is

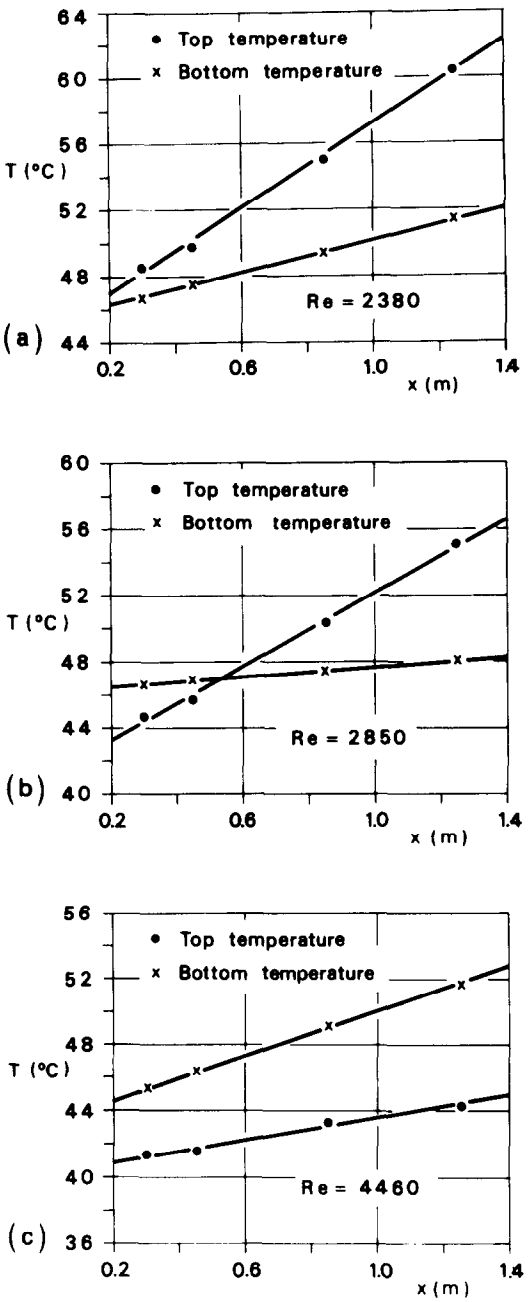

FIG. 3. Longitudinal distributions of top and bottom inner tube temperatures for $Ra^* = 1.1 \times 10^8$ and $D_o/D_i = 1.65$: (a) $Re = 2380$, (b) $Re = 2850$, (c) $Re = 4460$.

characteristic of the intermediate Reynolds numbers. The intersection point moves downstream with increasing Re, and at larger values of Re, $T_b > T_t (Nu_b < Nu_t)$ for all x. In contrast, for the outer tube, the top temperature exceeds the bottom temperature at all longitudinal stations for the complete ranges of Re and Ra^*, although the temperature difference, $[T_{w,o}(\theta = 0°) - T_{w,o}(\theta = 180°)]$, decreases with increasing Re and decreasing Ra^*.

The trend associated with Figs. 3(a) and 4(a) is consistent with data previously obtained for

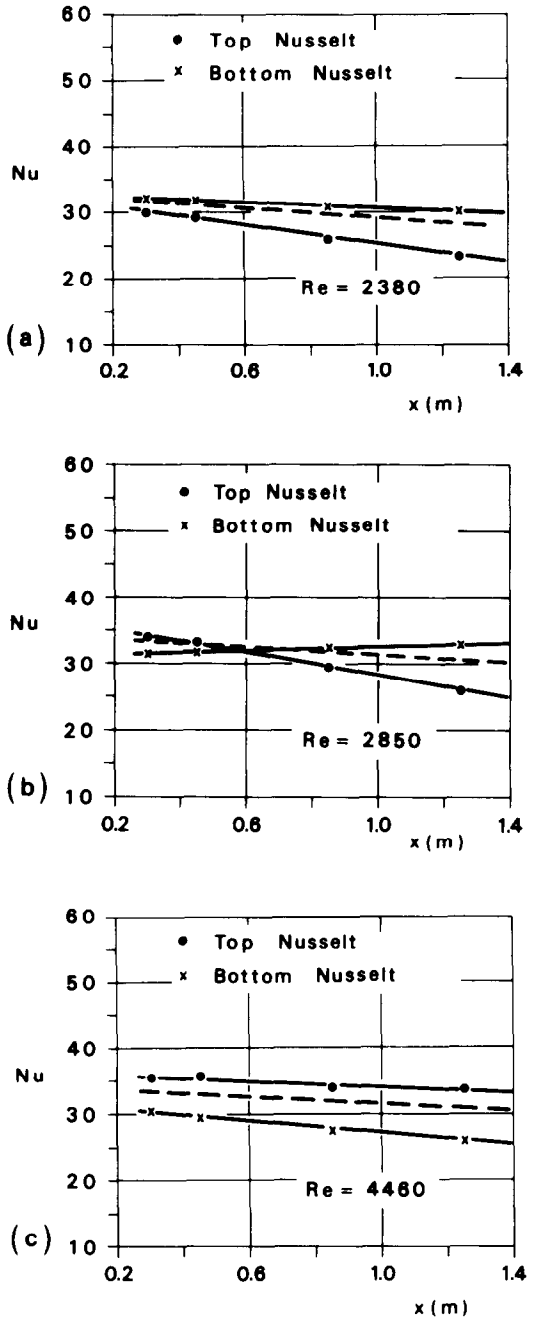

FIG. 4. Longitudinal distributions of the top, bottom, and circumferentially averaged (dashed line) inner tube Nusselt numbers for $Ra^* = 1.1 \times 10^8$ and $D_o/D_i = 1.65$: (a) $Re = 2380$, (b) $Re = 2850$, (c) $Re = 4460$.

$Re < 2200$ [7] and with numerical predictions obtained for laminar, mixed convection [3, 4]. Due to buoyancy effects, a thermal boundary layer forms on the inner tube at $\theta = 180°$ and grows as it ascends with decreasing θ along the tube surface. This behavior is similar to that observed for pure free convection boundary layer development on the inner tube of a concentric annulus [10], although in the present case superposition of the streamwise, forced convection flow induces a three-dimensional, helicoidal motion, rather than a two-dimensional, cellular motion. The existence of the helicoidal motion, which was suggested in a previous theoretical study [2], was confirmed by the flow visualization of this study. As shown by the streaklines in the sketch of Fig. 5(a), dye injected close to the inner tube at ($\theta = 180°$) rises along the tube surface in the upstream region. Some of the dye penetrates to the top of the annular gap in the mid and downstream regions, while the remainder follows a descending pattern, which is characteristic of helicoidal flow, and restores cooler fluid to the bottom of the inner tube. However, while the descending dye maintains an orderly streamline flow, motion of the dye in the top annular gap becomes irregular, suggesting a transition from laminar to turbulent flow.

From experimental studies of free convection in a concentric annulus, Kuehn and Goldstein [10] obtained results which are consistent with those found for the lower Reynolds number range of this study. In addition to obtaining values of $T_{w,i}(\theta = 0°) > T_{w,i}(\theta = 180°)$, they observed a transition from laminar to turbulent flow in the plume which ascended from the top of their heated inner tube. At Rayleigh numbers comparable to the lower limit of this study ($Ra^* \approx 10^7$), plume motion was characterized by spanwise oscillations. With increasing Rayleigh number, this motion became more irregular, until the entire plume became turbulent at Rayleigh numbers corresponding to the upper limit of their study ($Ra^* \approx 10^9$). However, even at $Ra^* \approx 10^9$, most of the inner cylinder boundary layer remained laminar. Note that it is the existence of the plume above the inner cylinder which causes $T_{w,o}(\theta = 0°)$ to exceed $T_{w,o}(\theta = 180°)$ for all of the conditions of this study.

Based upon the foregoing results it is concluded that, for smaller Reynolds numbers in the range of this study, laminar or near laminar flow conditions exist in all but the uppermost region of the annular passage. Although mixing within this region increases

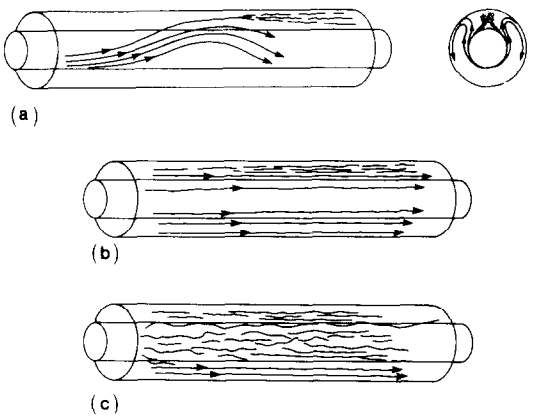

FIG. 5. Sketches of observed dye streaklines in horizontal annular flow for $Ra^* \approx 10^8$ and $0.3 < x < 0.7$ m: (a) $2200 < Re < 2500$, (b) $3500 < Re < 3800$, and (c) $4000 < Re < 4300$.

with increasing Rayleigh number, it is not sufficient to alter the effect which the buoyancy driven secondary flow has on supplying warm and cold fluid to the top and bottom, respectively, of the inner tube, and hence on maintaining $T_{w,i}(\theta = 0°) > T_{w,i}(\theta = 180°)$.

With increasing Reynolds number, there is a breakdown in the helicoidal nature of the flow around the inner cylinder. With this breakdown, circumferential (ascending and descending) velocity components are no longer comparable to the longitudinal components. This behavior is illustrated in Fig. 5(b), where the motion of dye injected at the top and bottom of the inner tube remains essentially in the longitudinal direction (no curved streamlines are evident along the side of the inner tube). Hence, the transport of warm fluid to the top of the inner tube by buoyancy driven advection is diminished. At Reynolds numbers approaching the upper range of this study, the flow became progressively more turbulent, although conditions remained laminar within that portion of the annular passage below the inner tube. The existence of turbulent flow in upper and side regions of the annulus is indicated in Fig. 5(c). The existence of laminar flow in the lower regions of the annulus was confirmed by measuring the fluid temperature with thermocouples traversed in the radial direction. While yielding significant temperature fluctuations for $\theta = 0°$, the measurements revealed negligible fluctuations for $\theta = 180°$.

The foregoing difference in flow conditions, which vary from laminar for $\theta = 180°$ to turbulent for $\theta = 0°$, is due to the effects of buoyancy. Above the inner tube, the natural turbulence of the flow is enhanced due to destabilizing temperature gradients induced by the heated tube. In contrast, below the inner tube, the stabilizing temperature gradient induced by the tube acts to attenuate turbulent fluctuations in the flow. The effect which the heated inner tube has on laminarizing the underlying flow is similar to that which has been observed for mixed convection beneath a heated horizontal plate [11].

The foregoing effects of Re may be used to interpret the trends revealed by Figs. 3(a)–(c). For smaller Reynolds numbers, laminar flow exists over most of the inner cylinder surface, and the helicoidal motion maintains a supply of warm water at the top of the cylinder and cold water to the bottom. With increasing Re the helicoidal flow is disrupted, reducing the upward flow of warm fluid over the cylinder surface, and turbulent flow is established over upper regions of the inner cylinder. For a fixed value of Ra^*, both of these effects act to significantly reduce $T_{w,i}(\theta = 0°)$. However, with increasing Re, laminar flow is maintained over lower regions of the inner cylinder, and reductions in $T_{w,i}(\theta = 180°)$ are less pronounced. Hence, with increasing Re, the significant downward shift in $T_{w,i}(\theta = 0°)$ causes the cross-over depicted in Fig. 3(b) and the inversion ($T_b > T_t$) of Fig. 3(c). The related flows are complicated by the coexistence of three-dimensional, laminar and turbulent conditions. Although measurements were not made for $Re > 5000$, further increases in Re would eventually produce a two-dimensional turbulent flow (with negligible buoyancy) over the entire annulus, and T_t would approach T_b.

Table 1. Mean, top and bottom longitudinal velocities for selected operating conditions

Re	$Ra^* \times 10^{-7}$	u_m(cm s^{-1})	u_t/u_m	u_b/u_m
2040	0	7.75	1.42	1.42
2300	9.60	9.12	1.43	1.69
3100	9.60	12.4	1.31	1.52
3780	9.60	15.2	1.19	1.36
4520	9.60	18.1	1.17	1.30

Measurements of $T_{w,i}$ have been made at other locations on the circumference of the inner tube. At all longitudinal stations, the measurements revealed a monotonic decay in $T_{w,i}$ with increasing θ for the conditions of Fig. 3(a) and a monotonic increase in $T_{w,i}$ with θ for the conditions of Fig. 3(c). Opposite trends are associated with the dependence of Nu on θ. The circumferential average of the local Nusselt number is shown by a dashed line for the conditions of Fig. 4. An error of less than 3% is incurred if this average is assumed to be the arithmetic mean of the top and bottom values, $\overline{Nu} \approx (Nu_t + Nu_b)/2$. Note that, although $\overline{Nu}$ decreases with increasing x over the range $0.3 < x < 1.4$ m, differences are less than the $\pm 10\%$ uncertainty in the measurements. Hence, to within this uncertainty, $\overline{Nu}$ may be assumed to be independent of x and the correlation of equation (3) is justified.

Longitudinal velocities inferred from the dye injection are listed in Table 1 for representative operating conditions. The mean velocity was obtained from a turbine flow meter, while the top and bottom velocities were obtained by tracking droplets injected midway between the two tubes at $\theta = 0°$ and 180°, respectively. Confidence in the tracking procedure is established by the fact that, for $Re = 2040$ and $Ra^* = 0$, $u_t = u_b$ and u_t/u_m is close to the maximum value of u/u_m associated with fully developed laminar flow. With $Ra^* > 0$, u_t is consistently smaller than u_b, confirming the existence of varying flow conditions at the top and bottom. The existence of smaller longitudinal velocities at the top is consistent with the laminar, mixed convection predictions of Kaviany [3], suggesting that the trend is due to the resistance to streamwise motion which is imposed by buoyancy driven flows above the inner cylinder. However, with turbulent flow at the top of the inner cylinder, it is more likely that the trend is due to dissipation of axial momentum by the turbulence.

Attempts have been made to correlate data for the relative magnitudes of Nu_t and Nu_b. Results obtained

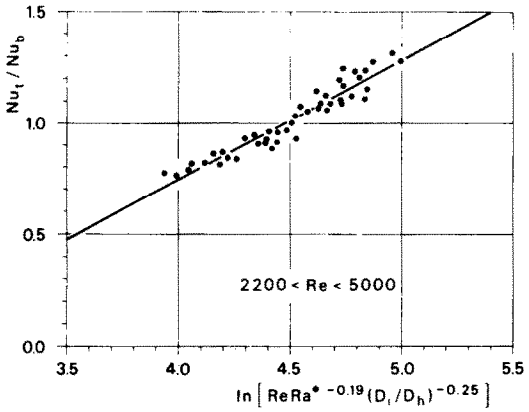

FIG. 6. Ratio of top and bottom Nusselt numbers for $x = 0.7$ m, $2200 < Re < 5000$, $10^7 < Ra^* < 10^9$, and $D_o/D_i = 1.65, 2.18$.

at $x = 0.70$ m for the entire range of operating conditions are shown in Fig. 6. The data are correlated by the expression

$$\frac{Nu_t}{Nu_b} = -1.41 + 0.537 \ln [Re\, Ra^{*-0.19}(D_i/D_h)^{-0.25}] \tag{4}$$

which indicates an increasing ratio with increasing Re and decreasing Ra^* and (D_i/D_h). This expression may be used to determine the Reynolds number Re_1 for which $Nu_t = Nu_b$. Setting Nu_t/Nu_b equal to unity and solving for Re, it follows that

$$Re_1 = 88.9 Ra^{*0.19}(D_i/D_h)^{0.25} \tag{5}$$

in which case

$$\frac{Nu_t}{Nu_b} = 1 + 0.537 \ln \frac{Re}{Re_1}. \tag{6}$$

The r.m.s. deviation of the data from equation (6) is 1%. From the previous flow visualization, it was found that the longitudinal station for which $Nu_t/Nu_b = 1$ corresponds approximately to that for which there is a breakdown in the aforementioned helicoidal flow.

Since Re_1 and Nu_t/Nu_b also depend on x, attempts were made to obtain a more general correlation of $Nu_t Nu_b$, which applies over a range of longitudinal positions. An expression which correlates data for $x = 0.4, 0.7$ and 1 m to within an r.m.s. deviation of 2% was obtained and is of the form

$$\frac{Nu_t}{Nu_b} = 1 + m(x/D_i) \ln \frac{Re}{Re_1} \tag{7}$$

where

$$m(x/D_i) = 2.11 \times 10^{-3}(x/D_i) + 0.492 \tag{8}$$

$$Re_1 = f(x/D_i) Ra^{*g(x/D_i)}(D_i/D_h)^{0.25} \tag{9}$$

$$f(x/D_i) = 1150 \exp(-0.124 x/D_i) \tag{10}$$

and

$$g(x/D_i) = 0.00733(x/D_i) + 0.0383. \tag{11}$$

The data and the correlation are plotted in Fig. 7, and the correlation has been verified for other locations in the range of $0.2 < x < 1.2$ m.

SUMMARY

Experiments have been perfomed to determine mixed convection flow and heat transfer in a horizontal, concentric tube annulus. The diameter of the heated inner tube was fixed, and two diameters of the insulated outer tube were considered. The Reynolds number range ($2200 < Re < 5000$) would correspond to transitional flow in pure forced convection; while in pure free convection, the Rayleigh number range ($10^7 < Ra^* < 10^9$) would correspond to laminar boundary layer development on the inner cylinder and a turbulent plume above the cylinder.

Flow visualization revealed complicated, three-dimensional conditions for which turbulent flow existed at the top of the annular region, while laminar flow was maintained at the bottom. For Reynolds numbers approximately less than a critical value Re_1,

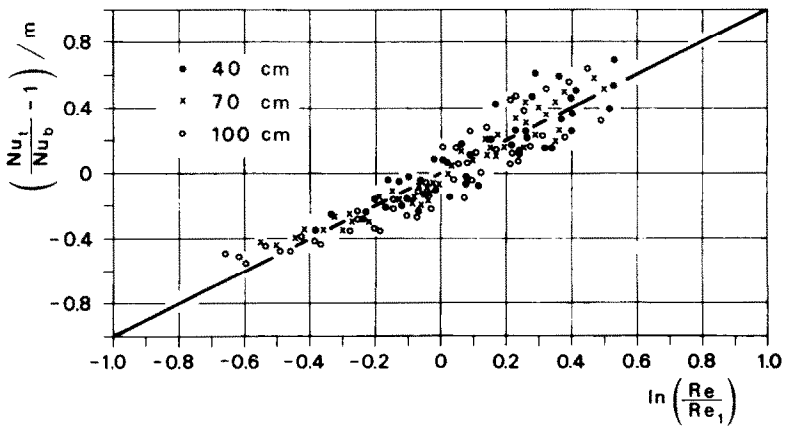

FIG. 7. Ratio of top and bottom Nusselt numbers for $x = 0.4$, 0.7 and 1.0 m; $2200 < Re < 5000$; $10^7 < Ra^* < 10^9$; and $D_o/D_i = 1.65, 2.18$.

flow along the sides of the annular region is laminar and helicoidal. The value of Re_1 increases with increasing Rayleigh number, Ra^*, and diameter ratio, D_i/D_h. With increasing $Re > Re_1$, the intensity of turbulence in the upper annular region increases and random fluctuations appear in the helicoidal flow as it undergoes transition to turbulence.

The heat transfer measurements reveal significant differences between local Nusselt numbers at the top and bottom of the inner cylinder, with differences depending upon the relative magnitudes of Re and Re_1. For $Re < Re_1$, the Nusselt number at the top of the cylinder exceeds that at the bottom, while the inverse is true for $Re > Re_1$. Correlations are provided for the ratio Nu_t/Nu_b. Although local Nusselt numbers depend upon longitudinal position in the duct, to within the uncertainty of the data, the circumferentially averaged Nusselt number may be assumed to be independent of x.

REFERENCES

1. N. Hattori, Combined free and forced-convection heat transfer for fully developed laminar flow in horizontal concentric annuli, *Heat Transfer—Jap. Res.* **8**, 27–48 (1979).
2. A. Mojtabi and J. P. Caltagirone, Analyse du transfert de chaleur en convection mixte laminaire entre deaux cylindres coaxiaux horizontaux, *Int. J. Heat Mass Transfer* **23**, 1369–1375 (1980).
3. M. Kaviany, Laminar combined convection in a horizontal annulus subject to constant heat flux inner wall and adiabatic outer wall, ASME Paper 84-WA/HT-49, Winter Annual Meeting, New Orleans, Louisiana (1984).
4. A. O. Nieckele and S. V. Patankar, Laminar mixed convection in a concentric annulus with horizontal axis, *J. Heat Transfer* **107**, 902–909 (1985).
5. S. Kotake and N. Hattori, Combined forced and free convection heat transfer for fully developed laminar flow in horizontal annuli, *Int. J. Heat Mass Transfer* **28**, 2113–2120 (1985).
6. N. Hattori and S. Kotake, Combined free and forced convection heat transfer for fully developed laminar flow in horizontal tubes, *Bull. J.S.M.E.* **21**, 861–868 (1978).
7. M. Ciampi, S. Faggiani, W. Grassi, F. P. Incropera and G. Tuoni, Experimental study of mixed convection in horizontal annuli for low Reynolds numbers, *Proc. Eighth International Heat Transfer Conf.*, San Francisco, California, Vol. 3, pp. 1413–1418 (1986).
8. V. T. Morgan, The overall convective heat transfer from smooth circular cylinders, *Advances in Heat Transfer* (edited by T. F. Irvine and J. P. Hartnett), Vol. 11, pp. 199–264 (1975).
9. G. D. Raithby and K. G. T. Hollands, A general method of obtaining approximate solutions to laminar and turbulent free convection problems, *Advances in Heat Transfer* (edited by T. F. Irvine and J. P. Hartnett), Vol. 11, pp. 266–317 (1975).
10. T. H. Kuehn and R. J. Goldstein, An experimental study of natural convection heat transfer in concentric and eccentric annuli, *J. Heat Transfer* **100**, 635–640 (1978).
11. D. G. Osborne and F. P. Incropera, Experimental study of mixed convection heat transfer for transitional and turbulent flow between horizontal parallel plates, *Int. J. Heat Mass Transfer* **28**, 1337–1344 (1985).

TRANSFERT THERMIQUE PAR CONVECTION MIXTE DANS UN ESPACE ANNULAIRE CONCENTRIQUE ET HORIZONTAL, POUR DES CONDITIONS D'ECOULEMENT DE TRANSITION

Résumé—Des expériences sont faites pour déterminer la convection mixte dans un espace annulaire entre tubes concentriques, horizontaux, pour des nombres de Reynolds dans le domaine $2200 < Re < 5000$. Dans ce domaine, les écoulements sont respectivement turbulent et laminaire dans les régions au-dessus et au-dessous du tube interne chauffé. Pour des nombres de Reynolds inférieurs à la valeur critique Re_1 qui dépend du nombre de Rayleigh, du rapport des diamètres et de la position longitudinale, l'écoulement le long des côtés de l'espace annulaire est laminaire et hélicoïdal. Pour $Re > Re_1$, il y a une rupture dans le mouvement hélicoïdal, avec transition à la turbulence au sommet et dans les régions latérales du passage annulaire. Le nombre de Nusselt local au sommet du tube intérieur est respectivement inférieur, égal et supérieur à celui à la base pour $Re < Re_1$, $Re = Re_1$ et $Re > Re_1$. Le nombre de Nusselt moyen sur la circonférence est faiblement dépendant de la position longitudinale et peut être exprimé en fonction des nombres de Rayleigh et de Reynolds, et du rapport des diamètres des tubes.

MISCHKONVEKTION IN HORIZONTALEN KONZENTRISCHEN RINGRÄUMEN IM ÜBERGANGSGEBIET DER STRÖMUNG

Zusammenfassung—Es wurden experimentelle Untersuchungen zur Bestimmung des Wärmeübergangs bei Mischkonvektion in einem horizontalen, konzentrischen Ringspalt, für Reynolds-Zahlen im Bereich von $2200 < Re < 5000$, durchgeführt. In diesem Bereich sind turbulente und laminare Strömungsbedingungen im Ringraum über bzw. unter dem beheizten inneren Rohr vorhanden. Für unterkritische Reynolds-Zahlen (kleiner als der Wert Re_1, welcher von der Rayleigh-Zahl, vom Durchmesserverhältnis und von der Position in Strömungsrichtung abhängt), ist die Strömung im Ringraum laminar und schraubenförmig. Für $Re > Re_1$ bricht die schraubenförmige Bewegung zusammen, und es folgt der Übergang zur Turbulenz im oberen und in den seitlichen Gebieten des Ringspaltes. Die örtliche Nusselt-Zahl auf der Oberseite des inneren Rohres ist kleiner ($Re < Re_1$), gleich ($Re = Re_1$) oder größer ($Re > Re_1$) als auf der Unterseite. Die über dem Umfang gemittelte Nusselt-Zahl hängt nur gering von der Position in Strömungsrichtung ab; sie wurde als Funktion von Rayleigh- und Reynolds-Zahl sowie vom Durchmesserverhältnis korreliert.

СМЕШАННОКОНВЕКТИВНЫЙ ТЕПЛОПЕРЕНОС В ГОРИЗОНТАЛЬНЫХ КОНЦЕНТРИЧЕСКИХ КОЛЬЦЕВЫХ КАНАЛАХ ПРИ УСЛОВИЯХ ПЕРЕХОДНОГО РЕЖИМА ТЕЧЕНИЯ

Аннотация—Проведены эксперименты по определению течения в условиях смешанной конвекции и теплопереноса в горизонтальном кольцевом канале для чисел Рейнольдса от 2200 до 5000. В этом диапазоне режим течения является турбулентным и ламинарным, соответственно, в зонах канала над и под нагреваемой внутренней трубой. Для чисел Рейнольдса, меньших критического значения Re_1, зависящего от числа Рэлея, отношения диаметров и продольной координаты, течение вдоль стенок канала является ламинарным и винтовым. При $Re > Re_1$ происходит разрушение винтового движения с последующим переходом к турбулентному в верхних областях канала. Локальное число Нуссельта на вершине внутренней трубы меньше, равняется или больше локального числа Нуссельта на нижней образующей при $Re < Re_1$, $Re = Re_1$ и $Re > Re_1$, соответственно. Осредненное по окружности число Нуссельта слабо зависит от продольной координаты и может быть выражено корреляционной зависимостью, содержащей числа Рэлея, Рейнольдса и отношение диаметров канала.